



Investigation of Anisotropic Properties of Al 5052 Alloy Deformed by Cryorolling and Cryo-cross Rolling

Ruby Pant¹ · Amit Joshi² · Saurabh Gairola³ · B. Hulugappa⁴ · K. K. Yogesha⁴

Received: 20 March 2023 / Revised: 24 July 2023 / Accepted: 25 July 2023 / Published online: 14 August 2023
© ASM International 2023

Abstract

In present work, the effect of cryorolling (CR) and cryo-cross rolling (CCR) on mechanical behavior of Al 5052 alloy, such as tensile and anisotropic behavior, and the corresponding microstructural evolution were explored in detail. The uniaxial tensile testing was performed on Al 5052 alloy samples for all sample conditions, and the anisotropic properties (mechanical anisotropy and planar anisotropy) were examined for deformed Al 5052 alloy. The measured anisotropic properties values were then compared for solution-treated samples (base material), CR and CCR processed samples. The result clearly indicates that the anisotropic properties of CCR processed samples show much improvement compared to CR processed samples. The microstructural features of processed Al 5052 alloy were characterized by optical microscopy, scanning electron microscopy (SEM), and electron backscattered diffraction (EBSD). Both CR and CCR deformed texture of Al5052 was conquered by the mixture of copper and brass that results the deformation texture had a considerably effects on their recrystallization behavior. The presence of high density second phase particle in the region of fine grains amended the anisotropic properties of CCR processed samples can be attributed to the existence of bimodal microstructure due to the formation of ultrafine grains as well as the coarse grain structure in Al 5052 alloy.

Keywords Cryo-cross rolling · Al 5052 alloy · Scanning electron microscopy · Mechanical anisotropy · Planar anisotropy

Introduction

Aluminum 5052 is a non-heat treatable magnesium-based aluminum alloy [1, 2]. It has been used in a wide variety of applications, such as the naval industry and armour plates, owing to its remarkable characteristics such as its high weldability, corrosion resistance and good strength-to-weight ratio [3]. The Al 5052 alloy was developed as a replacement for the conventional Al 5083 alloy in armor and naval applications due to its superior mechanical properties and corrosion resistance [3]. Apart from naval and armor plate

applications, Al 5052 alloy is popularly used in applications that require material in the form of structural frames and panels. This structural application, specifically in the automobile sector, takes advantage of the high specific strength of the aluminum alloys, which has a significant contribution in enhancing the fuel efficiency of the vehicle. Hence, the continuous efforts of the researchers have been focused on finding the routes/methods to achieve the materials in the form of highly strengthened sheets with a good amount of ductility and formability.

Since Al 5052 is a non-precipitation hardened alloy, its mechanical properties cannot be improved using the conventional heat treatment for aluminum alloys. Solid solution strengthening and strain hardening were identified as the keyways to enhance the strength of Al 5052 alloy. The high concentration of Mg (2.2–2.8%) is the main contributing factor to the high tensile strength observed in the Al 5052 alloy. Although Mg is soluble in Al and the large content of Mg in Al alloy can have a negative consequence on ductility and corrosion resistance [4, 5]. The mechanical characteristics, such as tensile strength, can be further enhanced using strain hardening and grain boundary strengthening, as observed by

✉ Amit Joshi
amitiitrebsd@gmail.com

¹ Mechanical Engineering Department, Uttarakhand University, Dehradun, India

² Mechanical Engineering Department, G. B. Pant Institute of Engineering and Technology, Pauri, India

³ Department of Engineering Design, Indian institute of technology, Madras, Chennai, India

⁴ Department of Mechanical Engineering, The National Institute of Engineering, Mysuru, India

the Hall-Petch equation. In continuation to this, the researchers have developed several severe plastic deformation (SPD) techniques that can improve mechanical properties using these two mechanisms (strain hardening and grain boundary strengthening) such as accumulative roll bonding (ARB) [6, 7], multi-axial forging (MAF) [8, 9] and cryorolling (CR) [10–12].

Rangaraju et al. [13] have reported a significant enhancement in the tensile strength of commercially pure aluminum by the formation of UFG structure using CR method. Similarly, Yogesha et al. [2] also observed an increase in the ultimate tensile strength of Al 5052 alloy after cryorolling treatment however this increase in the tensile strength is accompanied by a simultaneous decrease in ductility. A similar observation was made by Panigrahi et al. [14] in Al 6063 alloy that the enhancement in mechanical properties like tensile strength and hardness comes at the expense of ductility. Anas et al. [15] investigated the effect of cryorolling on tensile behavior and observed a slight increase of 11.15% in 30% cryorolled sample. This increase in mechanical properties was attributed to the combined effect of grain refinement, and dislocation strengthening. Similar observation regarding the strengthening mechanism was also made by Sekhar et al. [16] for 50% cryorolled Al 5052 alloy. Therefore, it is also expected that the formability of CR processed samples to be low. The researcher has shown that the ductility of CR processed samples can be increased by post-rolled annealing or aging treatment [17, 18]. Among all the SPD techniques, the CR process is one of the most important and significant SPD process due to its unique advantages like higher production yield, no special equipment required, no expensive tools required, and it can be up-scaled to a continuous mass production level. CR process is relatively simple, as well as the inexpensive SPD technique which can be used to produce UFG microstructure in various Al alloys [7], and it has the additional benefit of producing output in sheet form as required in many applications. The CCR or cryo-cross rolling is a modification of the original CR method in which the workpiece is rotated by 90° between each pass. The CCR has the additional advantage of improving the ductility of the metal along with the increase in strength. In CCR method, the advantage of cross-rolling associated with CR helps in achieving improved mechanical characteristics under diverse conditions. The mechanical behavior and microstructural evolution of different metals subjected to CCR have been explored by researchers [19]. However, studies on the anisotropy observed in the CCR and CR process are scarce in the literature.

Past studies reveal that very few researchers have investigated the anisotropic properties (mechanical anisotropy and planar anisotropy) of CR and CCR processed samples.

The mechanical properties obtained were correlated with the microstructural observation made using different characterization techniques such as optical microscopy, scanning electron microscopy and electron backscattered diffraction. The mechanical properties and the anisotropy evaluated in the current study can be utilized for obtaining suitable applications for the CR and CCR Al 5052 alloy.

Experimental Procedure

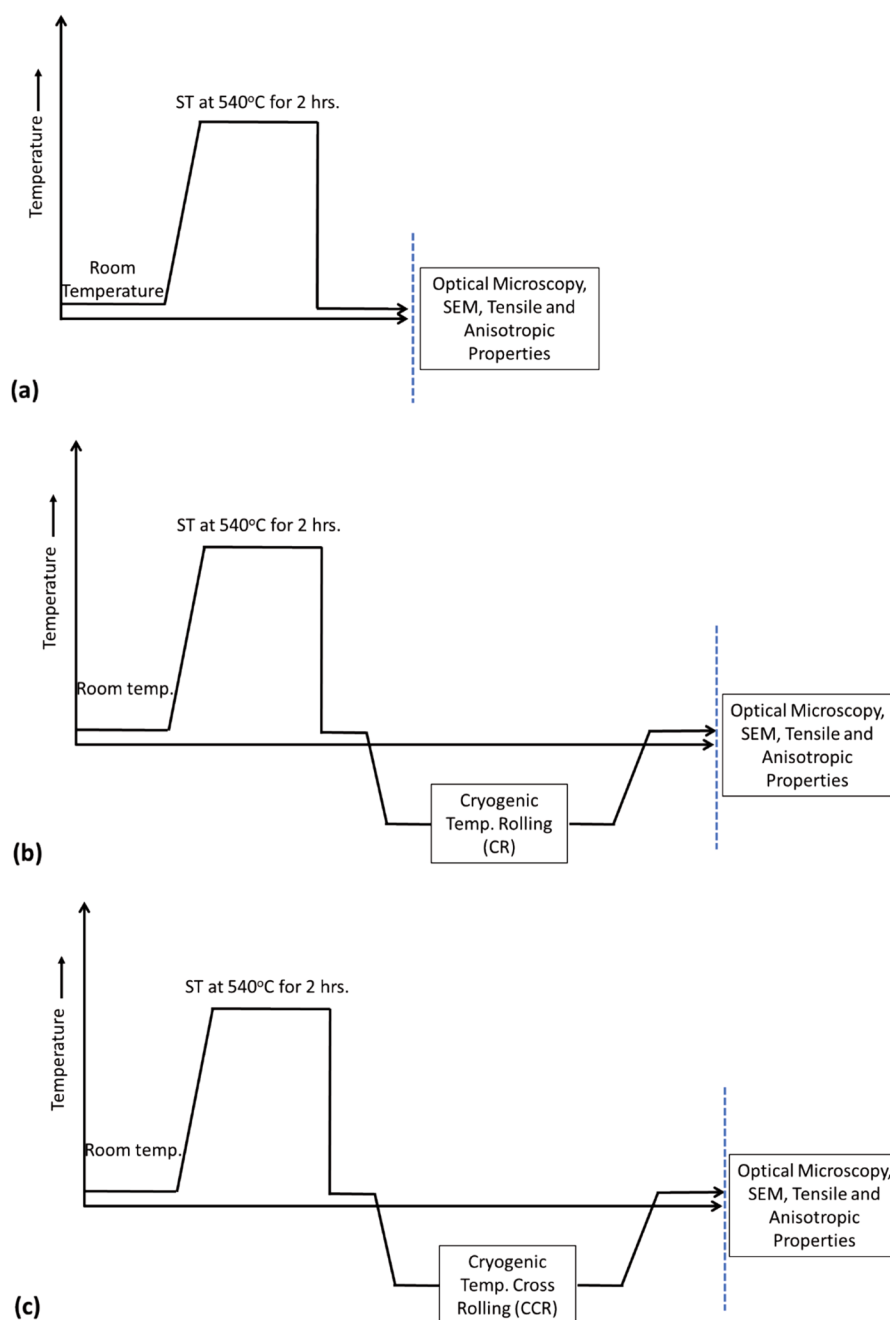
T6 tempered Al 5052 alloy in the form of 40 mm thick sheets was procured from BAM, Maharashtra, India. The samples with dimensions 40 mm × 30 mm × 10 mm were prepared from the as-received material. Then these samples were subjected to the solution treatment (ST) at the temperature of 540 °C for 2 hrs and followed by quenching in water at room temperature. Table 1 shows the chemical composition of Al 5052 alloy. The procedure for the solution treatment process was obtained from the published literature [21]. The Fe in aluminum alloys is a trace element and an impurity in the aluminum. Fe has an adverse impact on the mechanical properties of the aluminum alloys as it can form brittle intermetallic compounds such as AlFe or AlFeSi [31]. Fe in small amount (0.5–0.9%) can slightly improve the tensile strength, fatigue strength and ductility of the aluminum alloys however it significantly decreases the ductility of material. Hence the Fe is not usually utilized for improving the mechanical properties of the aluminum alloys and is primarily an impurity which should be controlled to ensure the good mechanical properties in aluminum alloys. These ST-processed samples were taken as the base material condition for the present work. In CR process, the samples were dipped in liquid nitrogen for about 10 minutes before each rolling pass, and the CCR process is similar to CR process except that after each pass of rolling, the material direction is rotated by 90°. In each rolling pass the thickness of the sample was reduced by 5% and the process was repeated till the thickness reduction of 90% (true strain of 2.3) was achieved. The CR and CCR samples were then annealed at a temperature of 100 °C for 45 min. The schematic line diagrams representing all the sample routes used in present study are shown in Fig. 1. The abbreviations used in the current studies are shown in Table 2.

The microstructure of CR and CCR processed samples was analyzed using optical microscopy (OM), scanning electron microscopy (SEM) and electron backscattered diffraction. The samples for microstructural characterization

Table 1 Chemical composition of the Al 5052 alloy (wt %)

Mg	Mn	Si	Fe	Cr	Cu	Ti	Zn	Al
2.8	0.1	0.25	0.4	0.25	0.1	0.15	0.1	Rest

Fig. 1 Line diagram representing (a) ST process route, (b) CR process route and (c) CCR process route



were prepared using a standard metallographic procedure which starts with the mechanical polishing of the sample using emery paper of grit size from 320 to 3000. Then the samples were polished using a colloidal silica solution of 0.5 μm . The OM samples were etched using Poulton's reagent and observed using the "Leica DMI 500" microscope. The samples for the EBSD test were then electropolished using an electrolyte consisting of perchloric acid and ethanol in a 90:10 ratio. The test was performed on the "FEI quanta 200 HV SEM microscope." The mechanical behavior of CR and CCR processed samples was evaluated

using tensile test. Tensile test samples were prepared from processed sheets along 0° , 45° , and 90° with respect to the rolling direction as per ASTM E8 sub-size standard (Dog bone shaped). The specifications of the tensile specimen are illustrated in Fig. 2. The test was performed on the "H25K-S Tinius Oslen machine" at the strain rate of $5 \times 10^{-4} \text{ s}^{-1}$, and the tests were repeated for three times in each processing condition. Anisotropic properties were identified by subjecting the specimens (marked along the gage length) to partial deformation (within an unvarying ductility range).

Table 2 Abbreviation used in the current manuscript

CR	Cryorolling
CCR	Cryo-cross rolling
OM	Optical microscopy
SEM	Scanning electron microscopy
EBSD	Electron backscattered diffraction
SPD	Severe plastic deformation
ARB	Accumulative roll bonding
MAF	Multi-axial forging
ST	Solution treatment
UTS	Ultimate tensile strength
YS	Yield strength
HAGB	High angle grain boundary
LAGB	Low angle grain boundary
IPF	Inverse pole figure
CR + AN _{100°C}	Cryorolled followed by annealing at 100 °C temperature
FCC	Face centered cubic
KAM	Kernel average misorientation
GND	Geometrically necessary dislocation

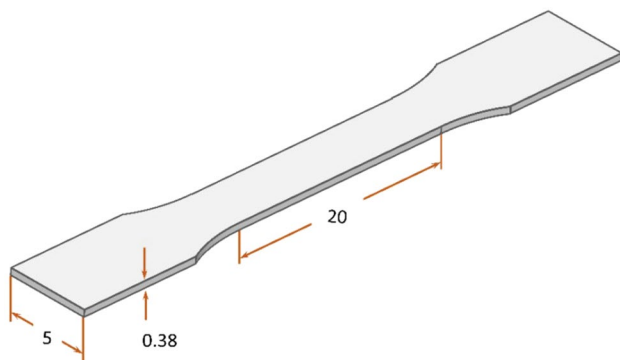


Fig. 2 Specification of the tensile specimen

Results and Discussion

Microstructural Characterization

Optical Microscopy

The microstructure of Al 5052 in different processing conditions, such as ST, CR, and CCR was characterized using optical microscopy. The optical micrographs of Al 5052 alloy for different processing conditions are shown in Fig. 3a–c. Figure 3a reveals that the ST process of Al 5052 alloy leads to the development of a uniformly distributed equiaxed microstructure with an average grain size of 200 μm. The grain size in different conditions was evaluated through the line intercept method. After CR and CCR process, the reduction in grain size takes place, and the grains become elongated along the rolling direction. Optical micrographs of CR-processed and CCR-processed Al 5052 alloy are depicted in Fig. 3b, c, respectively. The evolution of deformation substructures, such as cells after severe plastic deformation, such as CR and CCR, has been observed by several researchers for aluminum alloys [21, 22]. The width of grains in CCR processed Al 5052 alloy samples is larger when compared to the CR processed samples. In cross cryorolling the sample is rotated after each rolling pass, and this leads to more uniform deformation in the CCR sample. The uniform deformation in the CCR samples might be responsible for the broader grains observed in the CCR sample. The uniform deformation behavior was also observed by other researchers for different aluminum alloys such as Al-Cu-Li alloys [25], Al 2219 [26].

Electron Backscattered Diffraction (EBSD) Analysis

Inverse pole figure (IPF) map of the CR, CCR, CR + AN_{100°C} and CCR + AN_{100°C} samples is depicted in Fig. 4. The cryorolled and cross-cryorolled sample shows elongated grains

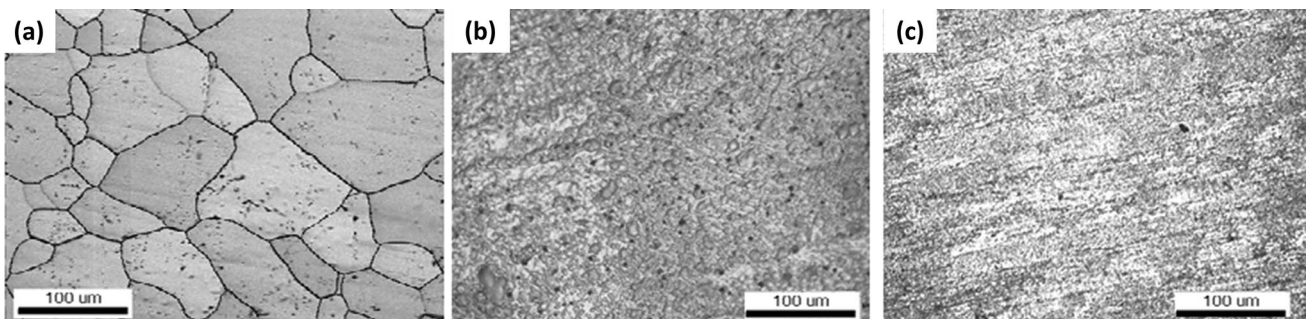


Fig. 3 Optical micrographs of Al 5052 alloy for (a) ST processed samples, (b) CR processed samples and (c) CCR processed samples

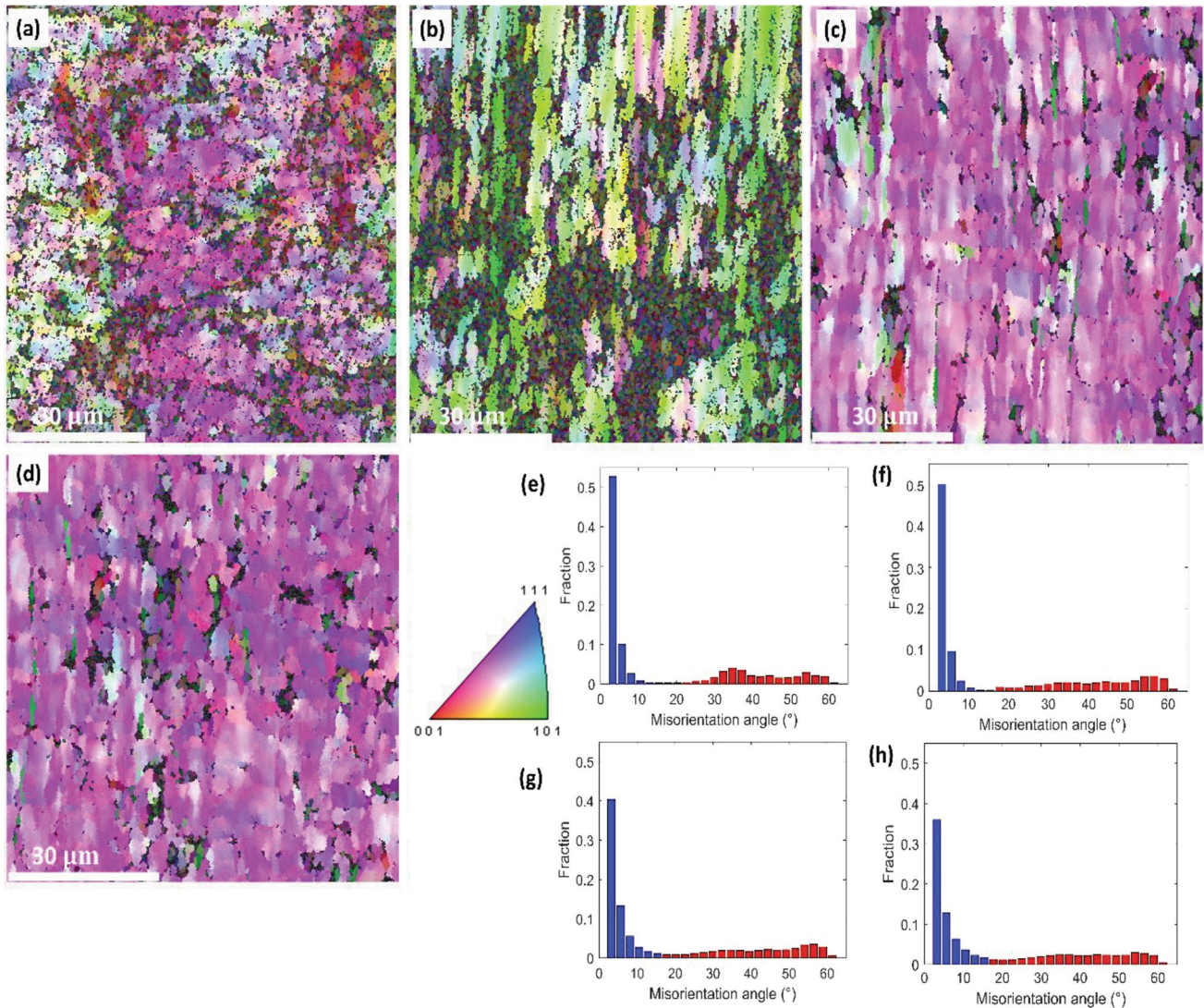


Fig. 4 Inverse pole figure (IPF) image of (a) CR (b) CCR (c) CR + AN_{100°C} (d) CCR + AN_{100°C}. Misorientation map for (e) CR (f) CCR (g) CR + AN_{100°C} (h) CCR + AN_{100°C}

with ultrafine-grained (UFG) microstructure, as illustrated in Fig. 4a, b, respectively. The cross-cryorolled sample shows a smaller average grain size of 0.42 μm compared to the cryorolled sample, which has an average grain size of 0.58 μm . The misorientation profile of the CR and CCR samples is shown in Fig. 4e, f, respectively. The high-angle grain boundaries (HAGB, boundaries with misorientation greater than 15°) are shown in red color in Fig. 4e–h, and the low-angle grain boundaries (LAGB, grain boundaries with misorientation angle between 2° and 15°) is shown by blue color. Both cryorolled and cross-cryorolled samples show a high fraction of low-angle grain boundaries with average misorientation of 18.2° and 18.6°, respectively. The high fraction of LAGB can be accredited to the formation of dislocation substructures, such as dislocation cells, sub-grains etc., in the CR and CCR samples. The fraction of

HAGB and LAGB in the different conditions is shown in Table 3. The fraction of HAGB is slightly higher in CCR compared to CR (0.368 in CCR compared to 0.332 in CR). The inverse pole figure (IPF) image of the CR + AN_{100°C} and CCR + AN_{100°C} samples are shown in Fig. 4c and d, respectively. The grain size of both cryorolled and cross-cryorolled samples increases after annealing treatment; however, the grains remain elongated. The average grain size of the CR + AN_{100°C}, and CCR + AN_{100°C}, samples were observed to be 0.84 μm and 0.75 μm , respectively. The fraction of the HAGB is improved after annealing treatment in both CR and CCR samples. The HAGB fractions in CR + AN_{100°C}, and CCR + AN_{100°C}, samples are 0.352 and 0.372, respectively, as indicated in Fig. 4g, h. The high-angle grain boundaries have higher resistance to slip due to their higher

crystallographic misalignment and hence are responsible for improving the strength of the material.

The IPF texture map along {001}, {110}, and {111} directions for CR, CCR, CR + AN_{100°C}, and CCR + AN_{100°C} samples are shown in Fig. 5(a-d). Both cryorolled and cross-cryorolled show a mixture of copper ({112} < 111 >) and brass texture ({011} < 211 >). The maximum intensity of the texture is observed to be higher in the CCR sample compared to the CR sample. The maximum texture intensity in CR and CCR samples is 13.63 and 14.64, respectively, as shown in Fig. 5a, b. The copper texture is usually formed in the high stacking fault energy FCC metals during rolling [27, 28]. In contrast, the brass texture is mainly prevalent in the low stacking fault energy FCC material [29]. The texture intensity is further increased after the heat treatment process to 21.55 in the CR sample and 26.06 in the CCR sample, as depicted in Fig. 5c, d.

The deformation in the cryorolled and cross-cryorolled conditions before and after annealing treatment is examined through kernel average misorientation and dislocation density. The kernel average disorientation or KAM map is an indicator of the GND (geometrically necessary dislocation) in a local area. The dislocation density was determined using the following equation [30]:

$$\rho_{\text{GND}} = \frac{k\gamma\theta}{\mu b}$$

where ρ_{GND} is the geometrically necessary dislocation, θ is the average KAM value, b is the burger vector, k is the correction factor, γ is the material constant which is 3 for the mixed type of boundaries. Both cryorolled and cross-cryorolled sample shows high dislocation density. However, the cross-cryorolled sample shows higher dislocation density compared to the cryorolled sample, as noticed from Fig. 6a–d. This might be due to more homogenous deformation in the CCR sample compared to the CR sample. The dislocation density in CR and CCR samples is 1.14×10^{15} and 1.25×10^{15} , respectively. The dislocation density is decreased after annealing treatment to 5.37×10^{14} in the CR sample and 6.34×10^{14} in the CCR sample, as given in Table 3.

Mechanical Behavior

Tensile Properties

The variation of the ultimate tensile strength (UTS) and yield strength (YS) of Al 5052 alloy subjected to ST, CR and CCR process along 0° to the rolling direction is shown in Fig. 7. Al 5052 alloy in the solution treated

Table 3 Comparison of microstructural characteristics in different condition

Parameter	CR	CCR	CR + AN _{100°C}	CCR + AN _{100°C}
Average grain size (μm)	0.58	0.42	0.84	0.75
HAGB fraction	0.332	0.368	0.352	0.372
LAGB fraction	0.668	0.632	0.648	0.628
Average misorientation	18.2°	18.6°	31.5°	33.8°
Average KAM	1.87	2.05	0.88	1.04
Dislocation density	1.14×10^{15}	1.25×10^{15}	5.37×10^{14}	6.36×10^{14}

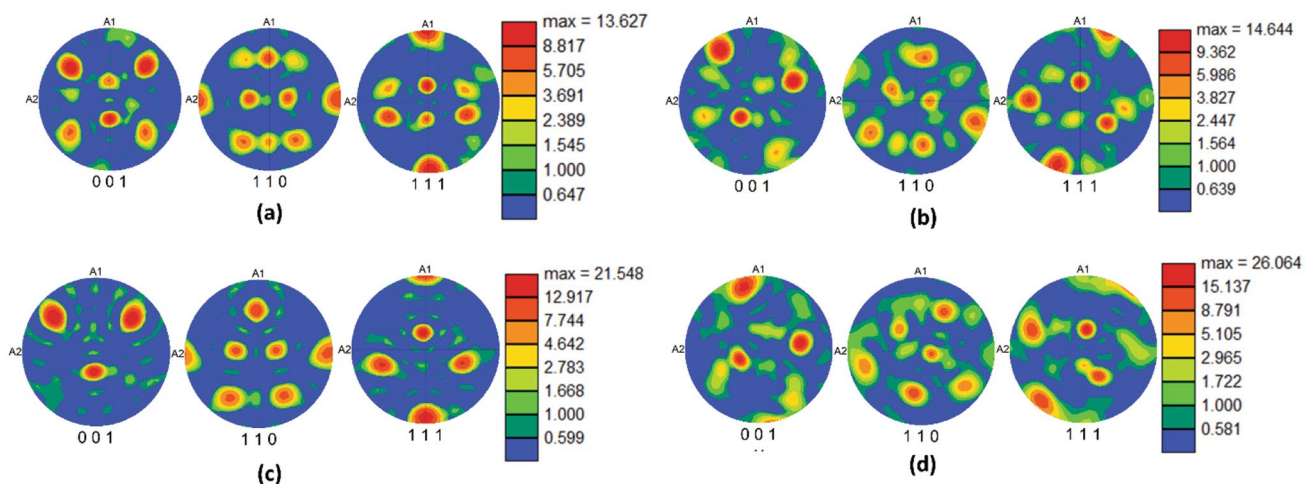
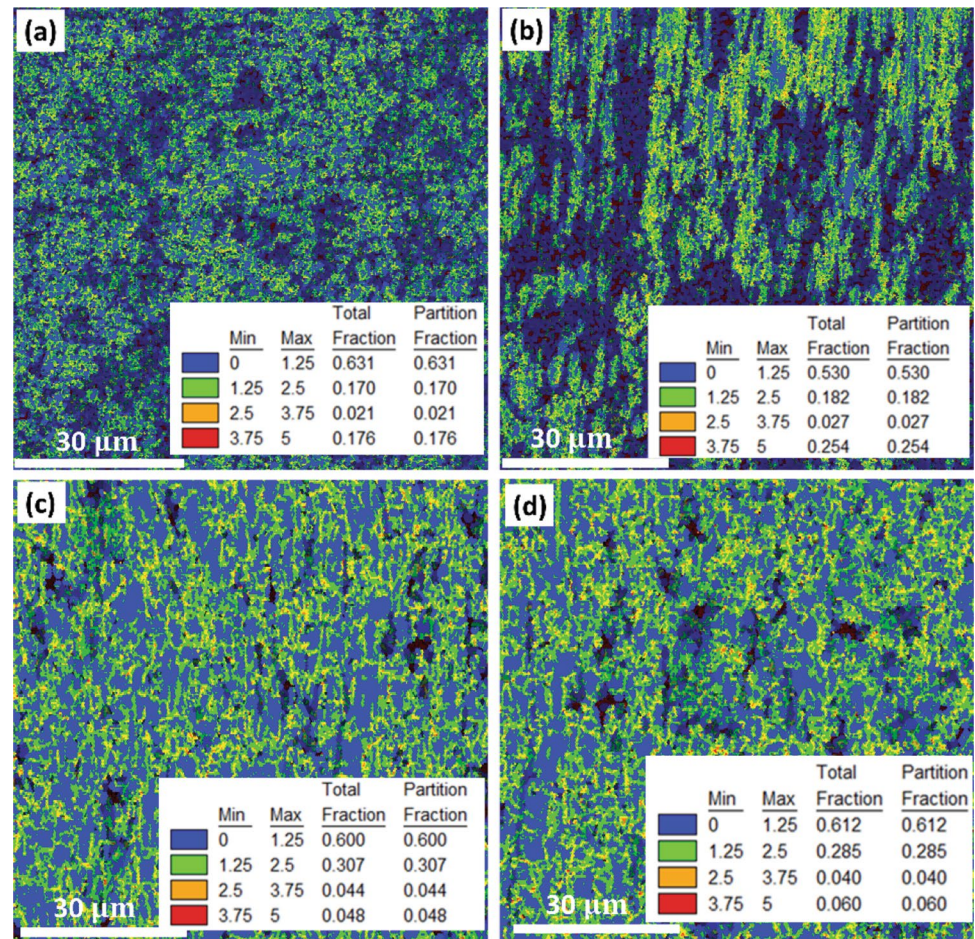


Fig. 5 Texture along {001}, {110}, and {111} for (a) CR (b) CCR (c) CR + AN_{100°C}, (d) CCR + AN_{100°C}

Fig. 6 Kernel average mis-orientation (KAM) of (a) CR (b) CCR (c) CR + AN_{100°C} (d) CCR + AN_{100°C}



(ST) condition possesses the YS of 80.84 MPa and UTS of 169.49 MPa. An enhancement of 94.35% in YS and 70.51% in UTS is observed for the samples deformed by the CR process. This enhancement in UTS and YS can be attributed to the suppression of dynamic recovery, which in turn results in high dislocation density of the CR sample [14]. CCR processed samples show further enhancement in YS value as 228.62 MPa and UTS value as 435.83 MPa. The mechanical properties, such as tensile and yield strength of the Al 5052 alloy, were observed to be highest for the CCR condition. These superior mechanical properties of the CCR sample can be accredited to better recrystallization, grain refinement, and dislocation strengthening in the CCR samples [25, 26].

Anisotropic Properties

The formability of sheets is an essential parameter for materials for different applications. Critical parameters such as mechanical anisotropy and planar anisotropy were identified as the benchmark for accessing the formability of sheets. Materials microstructural features like stored dislocation density, grain morphology and crystallographic texture are

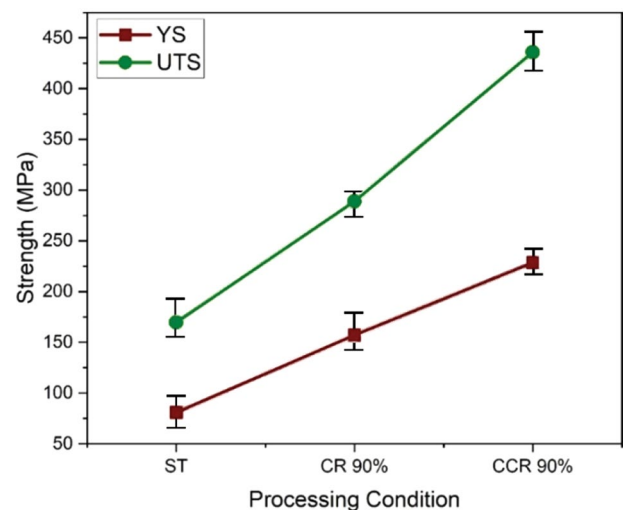


Fig. 7 Strength (YS and UTS) of Al 5052 alloy by ST, CR and CCR processed sheets along 0° to the rolling direction

the main factors that influence the value of mechanical and planar anisotropy [23, 24].

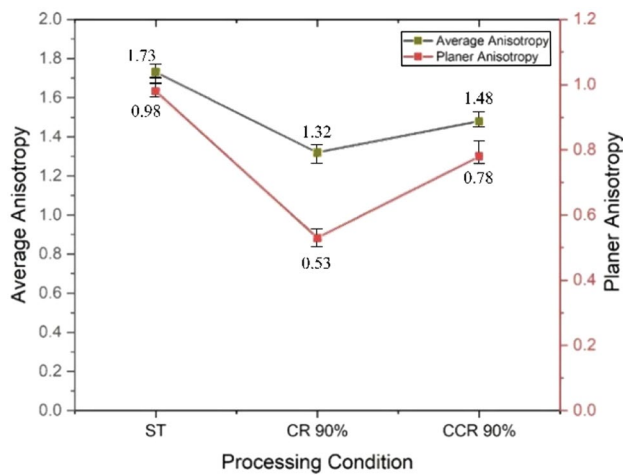


Fig. 8 Values of mechanical anisotropy and planar anisotropy for Al 5052 alloy processed through ST, CR and CCR process

Mechanical anisotropy (\bar{R}) is the measure of the resistance offered by sheet material to thinning of the sheet during forming, and it is calculated with the help of the following equation:

$$\bar{R} = \frac{R_0 + R_{45} + R_{90}}{4} \tag{1}$$

Planar anisotropy (ΔR) is the measure of the resistance offered by sheet material to the earing or bending of the sheet during forming, and it is calculated with the help of following equation:

$$\Delta R = \frac{R_0 - 2R_{45} + R_{90}}{2} \tag{2}$$

The Value of R_0 , R_{45} , and R_{90} was calculated with the help of following equation:

$$R_{0,45,90} = \left\{ \frac{\ln(w_0/w_f)}{\ln(l_f w_f / l_0 w_0)} \right\}_{0,45,90} \tag{3}$$

where w_0 , and w_f are initial and final width, and l_0 , and l_f are the initial and final lengths of the specimen. These are calculated by the average of the ratios between the true strain determined along length (l) and width (w) of tensile specimens oriented at various angles (0° , 45° , and 90°) to the rolling direction.

Based on equations (1), (2) and (3), the value of R and \bar{R} calculated and shown below in Fig. 8 for ST, CR and CR processed conditions.

Figure 8 clearly reveals that the value of \bar{R} for Al 5052 alloy is significantly higher for CCR processed sample compared to the CR processed sample. This indicates that the material processed through the CCR process possesses higher formability and can easily be deformed without thinning than the materials which are processed through the CR process. The higher formability of the CCR sample can be accredited to the uniform deformation as observed using the broader grain size in the optical micrograph in Fig. 3. Also, the value of ΔR for Al 5052 alloy is significantly higher for CCR processed sample when compared to the CR processed sample. This indicates the susceptibility of the Al 5052 alloy sheet (processed by CCR sample) to earing.

Fractography After Tensile Test

Figure 9(a)-(c) shows the fractographs of Al 5052 alloy after tensile test specimen for the ST, CR and CCR processed conditions. Figure 9(a) represents the ductile fracture of ST-processed samples because of the existence of primary and secondary dimples distributed all over the fractured surface. Figure 9(b) clearly reveals the existence of fine dimples along with the flat facets for CR processed samples and this

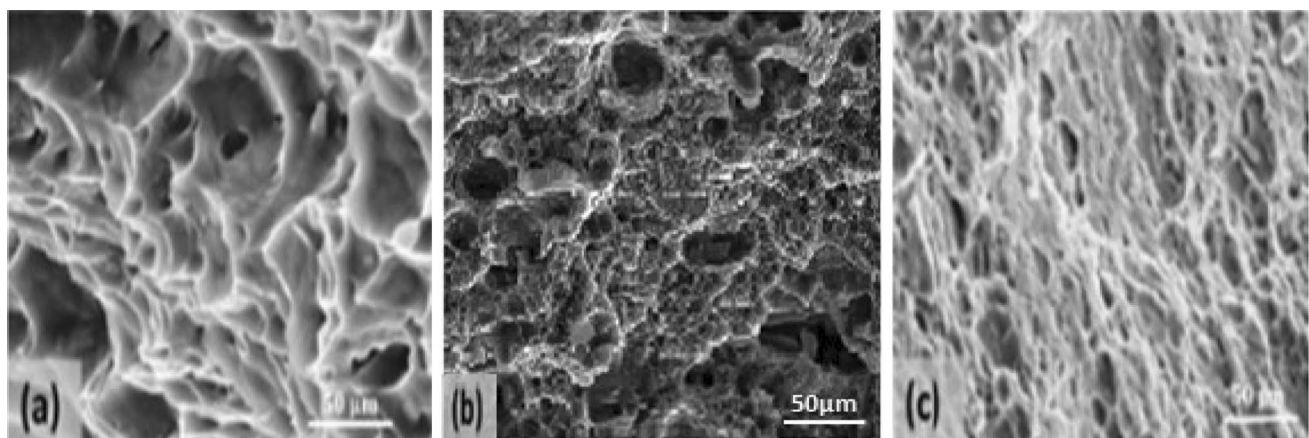


Fig. 9 Fractographs of Al 5052 alloy for (a) ST processed samples, (b) CR processed samples and (c) CCR processed sample

type of structure validates the grain refinement of Al 5052 alloy samples. Figure 9c shows that the fraction of fine dimpled structure is more along with the existence of flat facets for CCR processed Al 5052 alloy samples. Cross rolling improves the grain size of CR samples by recrystallization, and this has a direct consequence on dimple size obtained in SEM fractograph of tensile specimens. The mode of fracture in CR and CCR processed samples is observed to be a mixed mode fracture. This enhancement in the size of dimpled-grained structure is accompanied by a decrease in the density of areas with flat facets observed for the CCR processed samples and these changes depicts the higher tendency of CCR processed samples toward ductile fracture. In CR and CCR processed samples, the dimples size is significantly smaller compared to the ST processed samples, which clearly indicates the formation of UFG structure in CR samples.

Conclusion

The mechanical and anisotropic properties of Al 5052 alloy were explored for three different processing routes, i.e., ST, CR, and CCR. The strength (both YS and UTS) was observed to be higher in the CCR sample compared to other processing conditions. Furthermore, the mechanical anisotropy was observed to be more favorable for CCR conditions, which in turn signifies the higher formability of material produced through this process along with the superior strength of the material. Also, the planar anisotropy, which is the measure of resistance to earing for CCR processed samples, is higher along with the other improved mechanical properties like strength. The higher mechanical properties of the CCR sample compared to the CR sample can be primarily attributed to the more uniform deformation, higher dislocation density, and smaller grain size as observed by EBSD analysis.

References

1. W.A. Gooch, M.S. Burkins, R.J. Squillacioti, Ballistic testing of commercial aluminum alloys and alternate processing techniques to increase the availability of aluminum armor. In *23rd International Symposium on Ballistics*, Tarragona, Spain (2007).
2. K.K. Yogesha, A. Joshi, N. Kumar, R. Jayaganthan, Effect of cryo groove rolling followed by warm rolling (CGW) on the mechanical properties of 5052 Al alloy. *Mater. Manuf. Process.* **32**(12), 1336–1344 (2017)
3. K. Nima, Y. Peimaei, Lightweight materials (LWM) in transportation especially application of aluminum in light weight automobiles (LWA). In *International Conference on Interdisciplinary Studies in Nanotechnology*, pp. 1–22 (2020).
4. J. Amit, K.K. Yogesha, N. Kumar, R. Jayaganthan, Influence of annealing on microstructural evolution, precipitation sequence, and fracture toughness of cryorolled Al–Cu–Si alloy. *Metall. Microstruct. Anal.* **5**(6), 540–556 (2016)
5. G. Jenő, N.Q. Chinh, Z. Horita, T.G. Langdon, Effect of Mg addition on microstructure and mechanical properties of aluminum. *Mater. Sci. Eng. A.* **387**, 55–59 (2004)
6. G.S. Mahmoud, M. Malaki, M. Gupta, Accumulative roll bonding—a review. *Appl. Sci.* **9**(17), 3627 (2019)
7. Y. Saito, H. Utsunomiya, N. Tsuji, T. Sakai, Novel ultra-high straining process for bulk materials—development of the accumulative roll-bonding (ARB) process. *Acta Mater.* **47**(2), 579–583 (1999)
8. K. Rajat, R. Jayaganthan, S. Gairola, R. Verma, Improvement of fracture toughness of ultra fine grained Al–Li 8090 alloy processed through multi axial forging. *Mater. Res. Express.* **6**(8), 085064 (2019)
9. J. Amit, N. Kumar, K.K. Yogesha, R. Jayaganthan, S.K. Nath, Mechanical properties and microstructural evolution in Al 2014 alloy processed through multidirectional cryoforging. *J. Mater. Eng. Perform.* **25**(7), 3031–3045 (2016)
10. P. Ruby, S. Singh, A. Joshi, K. Joshi, K.K. Saxena, Mechanical performance and characteristics evaluation of material through cryo rolling process: a review. *Mater. Today Proc.* **62**(6), 3086–3096 (2022)
11. R.B. Singh, A. Joshi, A. Gupta, M.K. Pathak, Improvement of mechanical properties of cryorolled LM6 alloy. *Mater. Today Proc.* **44**, 2107–2111 (2021)
12. R. Shubham, B.S. Rawat, A. Gupta, M.K. Pathak, A. Joshi, P. Rawat, P.K. Pant, EBSD studies on cryorolled LM6 Al alloy. *Mater. Today Proc.* **44**, 1969–1974 (2021)
13. R. Nikhil, T. Raghuram, B.V. Krishna, K.P. Rao, P. Venugopal, Effect of cryo-rolling and annealing on microstructure and properties of commercially pure aluminium. *Mater. Sci. Eng. A.* **398**(1–2), 246–251 (2005)
14. P.S. Kumar, R. Jayaganthan, A study on the mechanical properties of cryorolled Al–Mg–Si alloy. *Mater. Sci. Eng. A.* **480**(1–2), 299–305 (2008)
15. N.M. Anas, B.K. Dhindaw, H. Zuhailawati et al., Effect of initial microstructure on properties of cryorolled Al 5052 alloy subjected to different annealing treatment temperatures. *J. Mater. Eng. Perform.* **27**, 6206–6217 (2018)
16. K.C. Sekhar, R. Narayanasamy, K. Velmanirajan, Experimental investigations on microstructure and formability of cryorolled AA 5052 sheets. *Mater. Des.* **53**, 1064–1070 (2014)
17. P.M. Kumar, A. Joshi, K.K.S. Mer, R. Jayaganthan, Mechanical properties and microstructural evolution of bulk UFG Al 2014 alloy processed through cryorolling and warm rolling. *Acta Metallurgica Sinica.* **32**(7), 845–856 (2019)
18. G. Saurabh, A. Joshi, G. Brijesh, R. Pankaj, V. Raviraj, Correlation of tensile properties and fracture toughness with microstructural features for Al–Li 8090 alloy processed by cryorolling and post-rolled annealing. *Trans. Indian Inst. Metals.* **72**(7), 1743–1755 (2019)
19. G.S. Kumar, N. Fuloria, D. Jayaganthan, R. Singh, I.V. Srivastava, D. Dey, G.K.N. Saibaba, Evaluating fracture toughness of rolled zircaloy-2 at different temperatures using XFEM. *J. Mater. Eng. Perform.* **25**(9), 4046–4058 (2018)
20. K.K. Yogesha, A. Joshi, R. Jayaganthan, Fatigue behavior of ultrafine-grained 5052 Al alloy processed through different rolling methods. *J. Mater. Eng. Perform.* **26**, 2826–2836 (2017)
21. A. Joshi, K.K. Yogesha, R. Jayaganthan, Influence of cryorolling and followed by annealing on high cycle fatigue behavior of ultrafine grained Al alloy. *Mater. Charact.* **127**(2017), 253–271 (2014)
22. K.K. Yogesha, K. Nikhil, J. Amit, R. Jayaganthan, S.K. Nath, A Comparative study on tensile and fracture behavior of Al–Mg

- alloy processed through cryorolling and cryo groove rolling. *Metallogr. Microstruct. Anal.* **5**(3), 251–263 (2016)
23. A. Dhal, S.K. Panigrahi, M.S. Shunmugam, Influence of alloy chemistry on the deformation behaviour and anisotropic properties of aluminium ultra-fine-grained thin sheets. In *Journal of Physics: Conference Series*, vol. 1063, no. 1, pp. 012067. IOP. (2018).
 24. H.L. Fan, D.N. Fang, Anisotropic mechanical properties of lattice grid composites. *J. Compos. Mater.* **42**(23), 2445–2460 (2008)
 25. L. Wang, Y. Xiao, C. Kong, Yu. Hailiang, Mechanical properties and microstructure evolution of an Al–Cu–Li alloy via cross cryorolling. *Int. J. Lightweight Mater. Manuf.* **5**(4), 431–439 (2022)
 26. K. Sivaprasad, B. Blessto, V. Muthupandi et al., Achieving superior strength and ductility combination through cryorolling in 2219 aluminum alloy. *J. Mater. Eng. Perform.* **29**, 6809–6817 (2020)
 27. N. Nayan, S. Mishra, A. Prakash, S.V.S.N. Murty, M.J.N.V. Prasad, I. Samajdar, Effect of cross-rolling on microstructure and texture evolution and tensile behavior of aluminium-copper-lithium (AA2195) alloy. *Mater. Sci. Eng. A.* **740**, 2–261 (2019)
 28. R. Pant, A. Joshi, S. Singh, A. Raturi, “Influence of cryo-cross rolling and post-rolled annealing on microstructure and high cycle fatigue properties of Al-5052 alloy. *Metallogr. Microstruct. Anal.* **2**, 56 (2021). <https://doi.org/10.1007/s13632-023-00961-3>
 29. M. Moghaddam, A. Zarei-Hanzaki, M.H. Pishbin, A.H. Shafieizad, V.B. Oliveira, Characterization of the microstructure, texture and mechanical properties of 7075 aluminum alloy in early stage of severe plastic deformation. *Mater. Charact.* **119**, 137–147 (2016)
 30. K. Li, J. Zhan, T. Yang, A.C. To, S. Tan, Q. Tang, H. Cao, L.E. Murr, Homogenization timing effect on microstructure and precipitation strengthening of 17–4PH stainless steel fabricated by laser powder bed fusion. *Addit. Manuf.* **52**, 102672 (2022)
 31. K. Cheol-Woo, Y. Hyo-Sang, J. Jae-Yeol, C. Jae-Ik, H. Sung-Kil, The effect of Fe addition on microstructure, mechanical properties and electric conductivity of the as-cast Al–Mg–Si alloys. *J. Nanosci. Nanotechnol.* **21**, 1915–1919 (2021)

Publisher's Note Springer Nature remains neutral with regard to jurisdictional claims in published maps and institutional affiliations.

Springer Nature or its licensor (e.g. a society or other partner) holds exclusive rights to this article under a publishing agreement with the author(s) or other rightsholder(s); author self-archiving of the accepted manuscript version of this article is solely governed by the terms of such publishing agreement and applicable law.